Probing Higgs width and top quark Yukawa coupling from $t\bar{t}H$ and $t\bar{t}t\bar{t}$ productions

Qing-Hong Cao,[1,2,3,*] Shao-Long Chen,[4,3,†] and Yandong Liu[1,‡]

[1]*Department of Physics and State Key Laboratory of Nuclear Physics and Technology,*
Peking University, Beijing 100871, China
[2]*Collaborative Innovation Center of Quantum Matter, Beijing 100871, China*
[3]*Center for High Energy Physics, Peking University, Beijing 100871, China*
[4]*Key Laboratory of Quark and Lepton Physics (MoE) and Institute of Particle Physics,*
Central China Normal University, Wuhan 430079, China

We demonstrate that four top-quark production is a powerful tool to constrain the top Yukawa coupling. The constraint is robust in the sense that it does not rely on the Higgs boson decay. Taking into account the projection of the $t\bar{t}H$ production by the ATLAS Collaboration, we obtained a bound on the Higgs boson width, $\Gamma_H \leq 2.57\Gamma_H^{\mathrm{SM}}$, at the 14 TeV Large Hadron Collider with an integrated luminosity of 300 fb^{-1}.

I. INTRODUCTION

Four years after the Higgs boson discovery we still know little about the Higgs boson width (Γ_H) and its couplings to fermions in the Standard Model (SM). For its smallness, the Higgs boson width cannot be measured directly from the line shape of the Higgs boson resonance. One way to determine Γ_H is through the $gg \rightarrow H \rightarrow ZZ$ channel by comparing the production rate in the vicinity of the Higgs resonance with the rate away from the resonance [1]. So far, only upper bounds are obtained; for example, the current bounds on Γ_H at a 95% confidence level are $\Gamma_H \leq (4.5 \sim 7.5) \times \Gamma_H^{\mathrm{SM}}$ by the ATLAS Collaboration [2] and $\Gamma_H \leq 5.4\Gamma_H^{\mathrm{SM}}$ by the CMS Collaboration [3]. Similarly, the top Yukawa coupling ($y_{Ht\bar{t}}$) is not directly measured yet, although the Higgs boson discovery indicates that the Higgs boson must interact with top quarks to generate Higgs-gluon-gluon effective coupling. The top Yukawa coupling can be measured in the rare $t\bar{t}H$ production on the condition that the Higgs boson decays exactly as in the SM. Precise information about the Higgs boson width and the top Yukawa coupling will help us to decipher the Higgs boson properties and also shed light on new physics (NP) beyond the SM. In this work we discuss the measurement of Γ_H and $y_{Ht\bar{t}}$ in the four top quark ($t\bar{t}t\bar{t}$) production and the $t\bar{t}H$ production at the Large Hadron Collider (LHC). We demonstrate that the combination of the two production channels imposes stringent bounds on Γ_H and $y_{Ht\bar{t}}$.

As reported by the ATLAS Collaboration [4], the signal strength of the $t\bar{t}H$ production process could be measured with an ultimate precision of about 20% at the 14 TeV LHC with an integrated luminosity ($\mathcal{L}$) of 300 fb^{-1}. Under the

narrow width approximation, the production cross section of $pp \rightarrow t\bar{t}H \rightarrow t\bar{t}xx$ is

$$\sigma(pp \rightarrow t\bar{t}H \rightarrow t\bar{t}xx)$$
$$= \sigma^{\mathrm{SM}}(pp \rightarrow t\bar{t}H \rightarrow t\bar{t}xx) \times \kappa_t^2 \kappa_x^2 \frac{\Gamma_H^{\mathrm{SM}}}{\Gamma_H}$$
$$\equiv \sigma^{\mathrm{SM}}(pp \rightarrow t\bar{t}H \rightarrow t\bar{t}xx) \times \mu_{t\bar{t}H}^{xx}, \qquad (1)$$

where $\kappa_t \equiv y_{Htt}/y_{Htt}^{\mathrm{SM}}$ and $\kappa_x \equiv y_{Hxx}/y_{Hxx}^{\mathrm{SM}}$ are the scaling factors of the Higgs couplings. The signal strength $\mu_{t\bar{t}H}^{xx}$, defined as

$$\mu_{t\bar{t}H}^{xx} \equiv \frac{\sigma}{\sigma^{\mathrm{SM}}} = \frac{\kappa_t^2 \kappa_x^2}{R_\Gamma} \quad \text{with} \quad R_\Gamma \equiv \frac{\Gamma_H}{\Gamma_H^{\mathrm{SM}}} \qquad (2)$$

is expected to be measured with uncertainties [4]

$$\bar{\mu}_{t\bar{t}H}^{\gamma\gamma} = 1.00 \pm 0.38, \qquad \bar{\mu}_{t\bar{t}H}^{ZZ} = 1.00 \pm 0.49,$$
$$\bar{\mu}_{t\bar{t}H}^{\mu\mu} = 1.00 \pm 0.74, \qquad \bar{\mu}_{t\bar{t}H}^{\mathrm{comb}} = 1.00 \pm 0.32, \quad (3)$$

at the 14 TeV LHC with $\mathcal{L} = 300$ fb^{-1}. Here $\bar{\mu}_{t\bar{t}H}^{\mathrm{comb}}$ refers to the result of combining multiple Higgs decay modes. The κ_t, κ_x, and Γ_H parameters in $\mu_{t\bar{t}H}$ are independent; therefore, one cannot determine them from the $t\bar{t}H$ production alone. Bounds on the κ_t, κ_x, and R_Γ could be derived from a global analysis of various Higgs boson productions and decays [4]. Nevertheless, it is still valuable to consider one specific channel to directly bound on the three parameters. Luckily, there is a large hierarchy among branching ratios of the Higgs decay modes. That ensures that we consider two special cases:

(i) $\Gamma_H \simeq \Gamma_H^{\mathrm{SM}}$: it is a good approximation for the $H \rightarrow \mu^+ \mu^-$ and $H \rightarrow \gamma\gamma$ modes, because modifications on those rare decays would not dramatically affect the total width. Thus, one can determine the bound on the product of κ_t and κ_x as

*qinghongcao@pku.edu.cn
†chensl@mail.ccnu.edu.cn
‡ydliu@pku.edu.cn

$$\kappa_t^2 \kappa_x^2 = \bar{\mu}_{t\bar{t}H}, \tag{4}$$

assuming other couplings of the Higgs boson are the same as the SM predictions.

(ii) $\kappa_x \simeq 1$: Higgs boson might decay into a pair of invisible particles and modify the total width. A bound on κ_t and R_Γ is

$$\frac{\kappa_t^2}{R_\Gamma} = \bar{\mu}_{t\bar{t}H}. \tag{5}$$

If the top quark Yukawa coupling could be directly measured or constrained in one particular Higgs production channel, then one can impose bounds on κ_x and R_Γ based on Eqs. (4) and (5), respectively. Below we show that the $t\bar{t}t\bar{t}$ production is a powerful tool to constrain the top Yukawa coupling.

II. COLLIDER SIMULATION

Figure 1 displays the representative Feynman diagrams of the $t\bar{t}t\bar{t}$ production, which occurs either through the gluon mediation, the electroweak gauge-boson mediation, or the Higgs boson mediation in the SM. We name the corresponding matrix elements as $\mathcal{M}_g$, $\mathcal{M}_{Z/\gamma}$, and $\mathcal{M}_H$. There are two advantages of the Higgs-induced $t\bar{t}t\bar{t}$ production: (i) no dependence on the Higgs boson width, (ii) the cross section proportional to the top quark Yukawa coupling to the fourth power, i.e.,

$$\sigma(t\bar{t}t\bar{t})_H \propto \kappa_t^4 \sigma^{\mathrm{SM}}(t\bar{t}t\bar{t})_H, \tag{6}$$

where $\sigma^{\mathrm{SM}}(t\bar{t}t\bar{t})_H$ denotes the SM production cross section. The not-so-small interferences among the three kinds of Feynman diagrams are also accounted for. Since the QCD and electroweak gauge interactions of top quarks have been well established, we consider that only the top Yukawa coupling might differ from the SM value throughout this work. As a result, the cross section of $t\bar{t}t\bar{t}$ production is

$$\sigma(t\bar{t}t\bar{t}) = \sigma^{\mathrm{SM}}(t\bar{t}t\bar{t})_{g+Z/\gamma} + \kappa_t^2 \sigma_{\mathrm{int}}^{\mathrm{SM}} + \kappa_t^4 \sigma^{\mathrm{SM}}(t\bar{t}t\bar{t})_H, \tag{7}$$

where
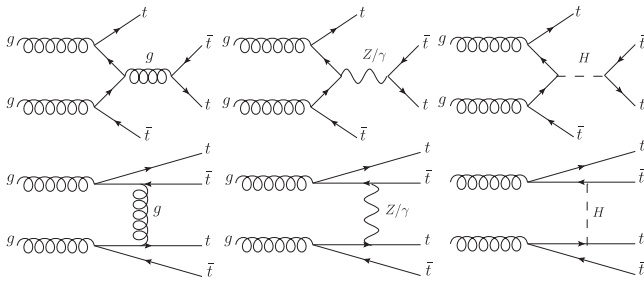
FIG. 1. Illustrative Feynman diagrams of $t\bar{t}t\bar{t}$ productions.

$$\begin{aligned}
\sigma^{\mathrm{SM}}(t\bar{t}t\bar{t})_{g+Z/\gamma} &\propto |\mathcal{M}_g + \mathcal{M}_{Z/\gamma}|^2 \\
&= |\mathcal{M}_g|^2 + |\mathcal{M}_{Z/\gamma}|^2 \\
&\quad + \mathcal{M}_g \mathcal{M}_{Z/\gamma}^\dagger + \mathcal{M}_g^\dagger \mathcal{M}_{Z/\gamma} \\
&= \sigma^{\mathrm{SM}}(t\bar{t}t\bar{t})_g + \sigma^{\mathrm{SM}}(t\bar{t}t\bar{t})_{Z/\gamma} \\
&\quad + \sigma^{\mathrm{SM}}(t\bar{t}t\bar{t})_{g+Z/\gamma,\mathrm{int}}, \\
\sigma^{\mathrm{SM}}(t\bar{t}t\bar{t})_H &\propto |\mathcal{M}_H|^2, \\
\sigma^{\mathrm{SM}}(t\bar{t}t\bar{t})_{\mathrm{int}} &\propto \mathcal{M}_{g+Z/\gamma} \mathcal{M}_H^\dagger + \mathcal{M}_{g+Z/\gamma}^\dagger \mathcal{M}_H. \tag{8}
\end{aligned}$$

As shown in the above equation, $\sigma^{\mathrm{SM}}(t\bar{t}t\bar{t})_{\mathrm{int}}$ denotes the interference between the Higgs mediation processes and the gluon and Z/γ mediation precesses. We use MadEvent [5] to calculate the leading order cross section of $t\bar{t}t\bar{t}$ production in the SM. The numerical results are summarized as follows:

	8 TeV	13 TeV	14 TeV
$\sigma^{\mathrm{SM}}(t\bar{t}t\bar{t})_{g+Z/\gamma}$:	1.344 fb,	9.997 fb,	13.140 fb,
$\sigma^{\mathrm{SM}}(t\bar{t}t\bar{t})_H$:	0.171 fb,	1.168 fb,	1.515 fb,
$\sigma^{\mathrm{SM}}(t\bar{t}t\bar{t})_{\mathrm{int}}$:	−0.224 fb,	−1.547 fb,	−2.007 fb.

$$\tag{9}$$

The numerical results shown above are checked with CalcHEP [6]. A highly integrated luminosity is needed to reach a 5σ discovery of the rare $t\bar{t}t\bar{t}$ production. However, null searching results in the low luminosity operation of the LHC are also useful because they can be used to constrain the top Yukawa coupling. For example, a 95% C.L. bound, $\sigma(t\bar{t}t\bar{t}) \leq 23$ fb, is reported by the ATLAS [7] and the CMS Collaborations [8] at the 8 TeV LHC. The upper limit of the $\sigma(t\bar{t}t\bar{t})$ is about 18 times larger than the SM theory prediction. That yields a bound of $\kappa_t \leq 3.45$ in terms of Eq. (7) and the tree-level cross section listed in Eq. (9). Recently, the CMS Collaboration updated their measurement of the four top quark production at the 13 TeV with an integrated luminosity of 2.6 fb^{-1}, yielding an upper limit of $\sigma(t\bar{t}t\bar{t})/\sigma(t\bar{t}t\bar{t})_{\mathrm{SM}} < 10.2$ [9]. That gives rise to an improved bound of $\kappa_t < 3.03$.

We notice that including higher order QCD corrections to the $t\bar{t}t\bar{t}$ production mildly affects the limit of κ_t. For example, we take the QCD corrections into account by introducing a constant K factor. Reference [10] calculated the next-leading order QCD corrections to the $t\bar{t}t\bar{t}$ production only through the gluon mediated channels and obtained a factor of $K_F = 1.27$. Since the interference term contains a QCD contribution as well, we multiply the tree-level cross section $\sigma(t\bar{t}t\bar{t})$ in Eq. (7) by a constant K factor of 1.27. The upper limit of κ_t changes from 3.45 to 3.25.

Next, we examine how well the top quark Yukawa coupling could be measured in the $t\bar{t}t\bar{t}$ production at the future LHC. A special signature of the $t\bar{t}t\bar{t}$ events is the

same-sign charged leptons (SSL) from the two same-sign top quarks. The ATLAS and CMS Collaborations have extensively studied the same-sign lepton pair signal at the LHC [11,12]. The other two top quarks are demanded to decay hadronically in order to maximize the production rate. Therefore, the topology of the signal event consists of two same-sign charged leptons, four b quarks, four light-flavor quarks, and two invisible neutrinos. In practice, it is challenging to identify four b jets. Instead, we demand that at least five jets are tagged and three of them are identified as b jets. The two invisible neutrinos appear as a missing transverse momentum ($\not{E}_T$) in the detector. Thus, the collider signatures of interests to us are two same-sign leptons, at least five jets with three of them tagged as b jets, and a large $\not{E}_T$.

The SM backgrounds for same-sign leptons can be divided into three categories: (i) a prompt same-sign lepton pair from the SM rare process, including the diboson and $W^\pm W^\pm jj$; (ii) a fake lepton, which comes from a heavy quark jet, namely b decays, and the dominant one is the $t\bar{t} + X$ events [13]; (iii) charge misidentification. As pointed out by the CMS Collaboration [12], the background from charge misidentification is generally much smaller and stays below the few-percent level. Thus, we ignore this type of background in our simulation and focus on those nonprompt backgrounds $t\bar{t} + X$ and rare SM processes contributions. For the four top quark production process, another feature worthy of being specified is that multiple b jets that decay from the top quark appear in the final state. Same-sign leptons, plus multiple b jets, have a significant discrimination with the backgrounds. Another SM process that can contribute to the same-sign lepton is the diboson production; however, it can be highly suppressed by the request of tagging multiple jets in the final state. Therefore, the major backgrounds are from the $t\bar{t} + X$ and $W^\pm W^\pm jj$ channels.

Both the signal and the background events are generated at the parton level using MADEVENT [5] at the 14 TeV LHC. The higher order QCD corrections are taken into account by multiplying the leading order cross sections with a next-to-leading-order K factor, e.g., $K_F = 1.4$ for the $t\bar{t}$ production [14,15], $K_F = 1.22$ for the $\bar{t}tW^+$ channel and $K_F = 1.27$ for the $\bar{t}tW^-$ channel [16], $K_F = 1.49$ for the $\bar{t}tZ$ production [17–22], and $K_F = 0.9$ for the $W^\pm W^\pm jj$ channel [23,24]. We use Pythia [25] to generate parton showering and hadronization effects. The DELPHES package [26] is used to simulate detector smearing effects in accordance to a fairly standard Gaussian-type detector resolution given by $\delta E/E = \mathcal{A}/\sqrt{E/\text{GeV}} \oplus \mathcal{B}$, where $\mathcal{A}$ is a sampling term and $\mathcal{B}$ is a constant term. For leptons, we take $\mathcal{A} = 5\%$ and $\mathcal{B} = 0.55\%$, and for jets we take $\mathcal{A} = 100\%$ and $\mathcal{B} = 5\%$. We require that the charged lepton has a transverse momentum p_T^ℓ greater than 20 GeV, rapidity $|\eta_\ell| \leq 2.5$, and its overlap with jets $\Delta R_{j\ell} = \sqrt{(\Delta\eta)^2 + (\Delta\phi)^2} \geq 0.4$. The $\not{E}_T$ is then defined to balance the total transverse momentum of visible objects.
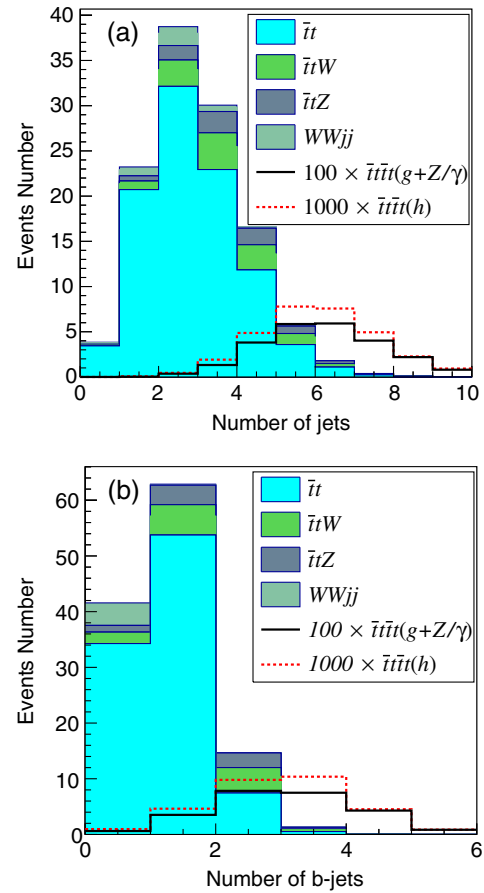
FIG. 2. The numbers of the reconstructed jets (a) and b-tagged jets (b) in the signal and background events at the 14 TeV LHC with an integrated luminosity of 1 fb^{-1}. To better characterize the signal distribution, the cross section has been rescaled to 1000 times. No cuts except for same-sign lepton pair have been applied.

Figure 2 displays the numbers of reconstructed jets (a) and b-tagged jets (b) in the signal and background processes. It is clear that the signal event often exhibits five or more jets. Demanding at least three identified b jets would efficiently reject those SM backgrounds. In the simulation we impose kinematics cuts listed as follows:

$$\begin{aligned}
\text{Basic}&: p_T^{j,\ell} \geq 20 \text{ GeV}, \qquad |\eta^{j,\ell}| < 2.5, \\
\text{SSL}&: N_{\ell^\pm} = 2, \\
\text{Jets}&: N_{\text{jets}} \geq 5, \qquad N_{b-\text{jets}} \geq 3, \\
\not{E}_T&: \not{E}_T \geq 100 \text{ GeV}, \\
m_T&: m_T \geq 100 \text{ GeV}, \\
H_T&: H_T \geq 700 \text{ GeV}.
\end{aligned} \qquad (10)$$

Here, m_T denotes the transverse mass of the leading charged lepton (ℓ_1) and the $\not{E}_T$, defined as

TABLE I.   The numbers of the signal and background events at the 14 TeV LHC with an integrated luminosity of 300 fb^{-1}. The kinematics cuts listed in each row are applied sequentially.

	Basic	SSL	Jets	E_T	m_T	H_T
$t\bar{t}t\bar{t}_H$	577.22	9.82	4.68	2.43	1.33	1.21
$t\bar{t}t\bar{t}_{g+Z/\gamma}$	5006.34	78.15	37.02	19.25	11.09	10.16
$t\bar{t}t\bar{t}_{\rm int}$	−764.67	−12.79	−6.19	−3.23	−1.93	−1.77
$t\bar{t}$	2.5×10^8	28802.4	44.1	18.9	0	0
$t\bar{t}W^+$	32670	2359.5	36.9	17.7	12.3	8.7
$t\bar{t}W^-$	16758	1397.1	49.5	9.9	4.5	4.5
$t\bar{t}Z$	24516	2309.4	20.1	10.8	10.8	9.3
$W^\pm W^\pm jj$	4187.7	1147.5	0.11	0	0	0

$$m_T = \sqrt{2p_T^{\ell_1} \slashed{E}_T (1 - \cos\Delta\phi)}, \qquad (11)$$

where $\Delta\phi$ is the azimuthal angle between the ℓ_1 lepton and the $\slashed{E}_T$. The m_T cut is to remove those backgrounds involving leptonically decayed W bosons. The H_T is the scalar sum of the transverse momenta of all the visible particles and the missing energy $\slashed{E}_T$.

Table I shows the numbers of the signal and the background events after a series of kinematics cuts at the 14 TeV LHC with an integrated luminosity of 300 fb^{-1}. The $t\bar{t}t\bar{t}$ production channels through the gluon, the electroweak gauge-boson, and the Higgs boson mediation share similar kinematics; therefore, all the $t\bar{t}t\bar{t}$ production channels exhibit similar efficiencies for each cut shown in Table I. The major backgrounds in the SM are from the $t\bar{t}W^\pm$ and $t\bar{t}Z$ productions. About 22.5 background events remain after all the cuts.

Next we discuss how well the top Yukawa coupling can be probed in the $t\bar{t}t\bar{t}$ production at the future LHC. As there are few events of both the signal and the backgrounds after the kinematics cuts, we obtain a 2σ exclusion limit on the $t\bar{t}t\bar{t}$ production rate using [27]

$$\sqrt{-2\left[n_b \ln\left(\frac{n_s + n_b}{n_b}\right) - n_s\right]} = 2, \qquad (12)$$

where n_s and n_b are the numbers of signal and background events, respectively. If a null result is observed on top of the 22.5 background events, then the number of signal events cannot exceed 10.9, from which we obtain $\kappa_t \leq 1.34$ with $\mathcal{L} = 300$ fb^{-1} using Eq. (7) with a confidence level of 95%. Bounds for other integrated luminosities can be derived similarly, yielding $\kappa_t \leq 1.94$ for $\mathcal{L} = 100$ fb^{-1}. In our analysis, we focus on the $\kappa_t \geq 0$ region. The option of negative κ_t is forbidden by the current experiment constraints of $H\gamma\gamma$ coupling [28,29].
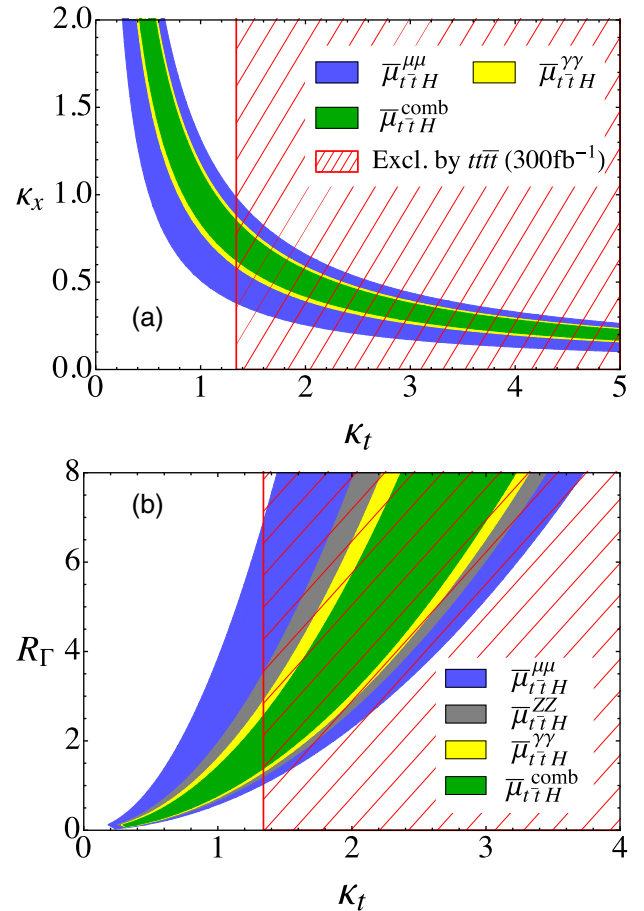
FIG. 3.   The relative uncertainty on the signal strength $\mu_{t\bar{t}H}$ projected in the plane of κ_t and κ_x (a) and in the plane of κ_t and R_Γ (b) at the 14 TeV with $\mathcal{L} = 300$ fb^{-1} for $H \to \gamma\gamma$ (yellow), $H \to \mu^+\mu^-$ (blue), $H \to ZZ$ (gray), and also the combination (green). The red meshed region is excluded by the $t\bar{t}t\bar{t}$ production with $\mathcal{L} = 300$ fb^{-1} with a 95% confidence level, respectively, if null signal events were observed.

Taking into account the $t\bar{t}H$ measurement projection at the 14 TeV LHC with $\mathcal{L} = 300$ fb^{-1}, one can derive a lower bound on κ_x and an upper bound on R_Γ. Figure 3 shows the relative uncertainty on the signal strength $\mu_{t\bar{t}H}$ projected in the plane of κ_t and κ_x (a) and in the plane of κ_t and R_Γ (b). The blue band represents the $t\bar{t}H$ measurement in the $H \to \mu^+\mu^-$ mode, the yellow band denotes the $H \to \gamma\gamma$ mode, and the gray band labels the $H \to ZZ$ mode. The green band is the result of combining different channels of the Higgs production and decay. See Eq. (3) for details. The red meshed regions are excluded by the $t\bar{t}t\bar{t}$ production with $\mathcal{L} = 300$ fb^{-1}, if null results were reported on top of the SM background.

First, we consider the correlation between κ_t and κ_x in the case of $\Gamma_H \simeq \Gamma_H^{\rm SM}$. In Fig. 3(a) we plot constraints on rare Higgs-decay modes, $H \to \gamma\gamma$ (yellow) and $H \to \mu\mu$ (blue), assuming that all of the Higgs couplings, except the top Yukawa coupling, are the same as in the SM. The κ_t exclusion limit derived from the $t\bar{t}t\bar{t}$ production requires that $\kappa_\mu \geq 0.38$ and $\kappa_\gamma \geq 0.59$ with $\mathcal{L} = 300$ fb^{-1}. The combination of multiple Higgs production channels yields a slightly tighter constraint.

Secondly, consider all of the Higgs couplings as in the SM, i.e., $\kappa_x = 1$. We obtain the correlation between κ_t and R_Γ shown in Fig. 3(b). The $\gamma\gamma$ (ZZ, $\mu^+\mu^-$) mode demands $R_\Gamma \leq 2.9$ (3.5, 6.9), respectively, at the 14 TeV LHC with $\mathcal{L} = 300$ fb^{-1}. The combination analysis demands $\Gamma_H \leq 2.6\Gamma_H^{\rm SM}$.

III. SUMMARY

In the article, we propose a novel method to measure the top quark Yukawa coupling in the $t\bar{t}t\bar{t}$ production.

The channel exhibits two advantages over other Higgs production channels: (i) the production cross section is proportional to κ_t^4 such that it is sensitive to the top quark Yukawa coupling; (ii) the channel is independent of the Higgs boson decay as only the off-shell Higgs boson are involved. Our simulation shows that a 95% confidence level limit of $\kappa_t < 1.94$ and $\kappa_t < 1.34$ could be obtained at the 14 TeV LHC with an integrated luminosity of 100 and 300 fb^{-1}, respectively.

The Higgs Yukawa coupling can also be measured in the $t\bar{t}H$ production, but it will be contaminated by the Higgs boson decay. Combining the $t\bar{t}t\bar{t}$ and $t\bar{t}H$ productions enables us to probe the correlation among the Higgs-Yukawa coupling and other Higgs properties, e.g., the total width and its couplings to the SM particles. Two special cases are considered in this article: (i) $\kappa_t^2\kappa_x^2 = \bar{\mu}_{t\bar{t}H}$ in the case of $\Gamma_H \simeq \Gamma_H^{\rm SM}$, i.e., the new physics (NP) effects only modifying the rare decays of the Higgs boson; (ii) $\frac{\kappa_t^2}{R_\Gamma} = \bar{\mu}_{t\bar{t}H}$ for $\kappa_x \sim 1$, i.e., the NP modifying the Higgs boson width sizably. If no deviation is observed in the $t\bar{t}t\bar{t}$ production at the 14 TeV LHC with an integrated luminosity of 300 fb^{-1}, then we obtain constraints on $\kappa_{\gamma,\mu}$ and Γ_H in the two cases: (i) $\kappa_\gamma > 0.59$ and $\kappa_\mu > 0.38$, (ii) $\Gamma_H < 2.6\Gamma_H^{\rm SM}$.

[1] F. Caola and K. Melnikov, Phys. Rev. D **88**, 054024 (2013).

[2] G. Aad *et al.* (ATLAS Collaboration), Eur. J. Phys. **75**, 335 (2015).

[3] V. Khachatryan *et al.* (CMS Collaboration), Phys. Lett. B **736**, 64 (2014).

[4] ATLAS Collaboration, CERN, Technical Report No. ATL-PHYS-PUB 016, 2014.

[5] J. Alwall, P. Demin, S. de Visscher, R. Frederix, M. Herquet, F. Maltoni, T. Plehn, D. L. Rainwater, and T. Stelzer, J. High Energy Phys. 09 (2007) 028.

[6] A. Belyaev, N. D. Christensen, and A. Pukhov, Comput. Phys. Commun. **184**, 1729 (2013).

[7] G. Aad *et al.* (ATLAS Collaboration), J. High Energy Phys. 08 (2015) 105.

[8] V. Khachatryan *et al.* (CMS Collaboration), J. High Energy Phys. 11 (2014) 154.

[9] L. Beck (CMS Collaboration), arXiv:1611.09607.

[10] G. Bevilacqua and M. Worek, J. High Energy Phys. 07 (2012) 111.

[11] ATLAS Collaboration, CERN, Technical Report No. AT-LAS-CONF 007, 2013.

[12] S. Chatrchyan *et al.* (CMS Collaboration), J. High Energy Phys. 01 (2014) 163; 01 (2015) 14.

[13] ATLAS Collaboration, CERN, Technical Report No. AT-LAS-CONF 105, 2012.

[14] V. Ahrens, A. Ferroglia, M. Neubert, B. D. Pecjak, and L. L. Yang, Phys. Lett. B **703**, 135 (2011).

[15] M. Czakon, P. Fiedler, and A. Mitov, Phys. Rev. Lett. **110**, 252004 (2013).

[16] J. M. Campbell and R. K. Ellis, J. High Energy Phys. 07 (2012) 052.

[17] A. Lazopoulos, T. McElmurry, K. Melnikov, and F. Petriello, Phys. Lett. B **666**, 62 (2008).

[18] M. V. Garzelli, A. Kardos, C. G. Papadopoulos, and Z. Trocsanyi, Phys. Rev. D **85**, 074022 (2012).

[19] A. Kardos, Z. Trocsanyi, and C. Papadopoulos, Phys. Rev. D **85,** 054015 (2012).

[20] M. V. Garzelli, A. Kardos, C. G. Papadopoulos, and Z. Trocsanyi, J. High Energy Phys. 11 (2012) 056.

[21] F. Maltoni, D. Pagani, and I. Tsinikos, J. High Energy Phys. 02 (2016) 113.

[22] S. Frixione, V. Hirschi, D. Pagani, H. S. Shao, and M. Zaro, J. High Energy Phys. 06 (2015) 184.

[23] B. Jager, C. Oleari, and D. Zeppenfeld, Phys. Rev. D **80,** 034022 (2009).

[24] T. Melia, K. Melnikov, R. Rontsch, and G. Zanderighi, J. High Energy Phys. 12 (2010) 053.

[25] T. Sjöstrand, S. Ask, J. R. Christiansen, R. Corke, N. Desai, P. Ilten, S. Mrenna, S. Prestel, C. O. Rasmussen, and P. Z. Skands, Comput. Phys. Commun. **191,** 159 (2015).

[26] J. de Favereau, C. Delaere, P. Demin, A. Giammanco, V. Lematre, A. Mertens, and M. Selvaggi (DELPHES 3), J. High Energy Phys. 02 (2014) 057.

[27] G. Cowan, K. Cranmer, E. Gross, and O. Vitells, Eur. Phys. J. C **71,** 1 (2011); **73,** 2501(E) (2013).

[28] G. Aad et al. (ATLAS, CMS), J. High Energy Phys. 08 (2016) 045.

[29] Q.-H. Cao, B. Yan, D.-M. Zhang, and H. Zhang, Phys. Lett. B **752,** 285 (2016).